Modeling Stratified Diffusion in Biological Invasions

Article *in* The American Naturalist · August 1995

DOI: 10.1086/285796

CITATIONS
441

READS
1,025

3 authors, including:

Nanako Shigesada

64 PUBLICATIONS **5,789** CITATIONS

SEE PROFILE

Kohkichi Kawasaki

Doshisha University

48 PUBLICATIONS **5,200** CITATIONS

SEE PROFILE

Modeling Stratified Diffusion in Biological Invasions

Nanako Shigesada; Kohkichi Kawasaki; Yasuhiko Takeda

The American Naturalist, Vol. 146, No. 2. (Aug., 1995), pp. 229-251.

Stable URL:
http://links.jstor.org/sici?sici=0003-0147%28199508%29146%3A2%3C229%3AMSDIBI%3E2.0.CO%3B2-5

The American Naturalist is currently published by The University of Chicago Press.

MODELING STRATIFIED DIFFUSION IN BIOLOGICAL INVASIONS

NANAKO SHIGESADA,[1,*] KOHKICHI KAWASAKI,[2,†] AND YASUHIKO TAKEDA[3,‡]

[1]Department of Information and Computer Sciences, Nara Women's University, Kita-Uoya Nishimachi, Nara 630, Japan; [2]Department of Knowledge Engineering and Computer Sciences, Doshisha University, Tanabe-cho, Kyoto 610-03, Japan; [3]Department of Biology, Kyushu University, Fukuoka 812, Japan

Submitted February 22, 1994; Revised September 14, 1994; Accepted October 5, 1994

Abstract.—Recent data on biological invasion show that range expansion is driven by various modes of dispersal such as neighborhood diffusion and long-distance dispersal that occur side by side within a species. In such a stratified dispersal process, the initial range expansion mainly occurs by neighborhood diffusion. However, as the range of the founder population expands, new colonies created by long-distance migrants increase in number to cause an accelerating range expansion in the later phase. We classify several well-documented examples of geographical expansions into three major types depending on the nonlinearity of the range-versus-time curve. To examine how long-distance dispersal produces accelerating range expansion, we construct a stratified diffusion model, which describes the dynamics of the size distribution of colonies created by long-distance migrants. The model consists of a von Foerster equation combined with a Skellam model. Analyzing the model provides an estimate of range expansion in terms of the rate of expansion due to neighborhood diffusion, the leap distance, and the colonization rate of long-distance migrants. The results explain various types of nonlinear range expansion observed in biological invasions.

Since Skellam's (1951) analysis of the data on the spread of the muskrat and his discovery that the square root of the area occupied by the population increases linearly with time, many models have been proposed that treat biological invasion as a combined process of Fickian diffusion and growth in population size (see reviews in Okubo 1980; Cliff et al. 1981; Murray 1989; Holmes et al. 1994). The ideas have been applied to a number of insects and mammals in an attempt to relate the rate of spread of populations to their behavioral and demographic properties (Lubina and Levin 1988; Okubo 1988; Andow et al. 1990, 1993). However, recent data on birds, insects, weeds, and even some mammals show that various modes of dispersal such as neighborhood diffusion and long-distance dispersal occur side by side within a species (Hengeveld 1989; Andow et al. 1990, 1993). Such species frequently exhibit nonlinear range-versus-time curves. It has been suggested that the initial speed of expansion is mainly determined by neighborhood diffusion of a founder population and that the accelerated expansion ob-

* To whom all correspondence should be addressed; E-mail: sigesada@ics.nara-wu.ac.jp.
† E-mail: kkawasak@doshisha.ac.jp.
‡ E-mail: ytakescb@mbox.nc.kyushu-u.ac.jp.

Am. Nat. 1995. Vol. 146, pp. 229–251.

served in the later phase is largely a reflection of the growth of new colonies successively created by long-distance migrants (Andow et al. 1993). Hengeveld (1989) proposed calling such a diffusion process "stratified diffusion." There have been a few attempts at mathematical modeling of stratified diffusion: Mollison (1977) dealt with dispersal by introducing redistribution kernels that incorporate various step lengths of dispersal, and Mack (1985) pointed out that multiple foci of new colonies accelerate the invasion as the number of foci is increased.

In this article, we reexamine several well-documented examples of geographical expansions with a view to gaining deeper insights into the relationship between the mechanism of dispersion and the spatiotemporal pattern of invasion. Invasion processes of these species generally involve three stages: establishment in the new habitat, range expansion, and saturation. The pattern of range expansion is further classified into three major types depending on nonlinearity of range-versus-time curves. We first show that the establishment phase can be interpreted by the conventional model originally introduced by Skellam. We then construct new models to deal with stratified diffusion. The models consist of a von Foerster equation combined with Skellam's model. Analysis of these equations gives the growth dynamics of a colony founded by a pioneering population and of offspring colonies expanding in isolation. We apply these results to the examples of biological invasions reviewed in this article and interpret how different types of range expansion arise from various combinations of short- and long-distance dispersals.

CLASSIFICATION OF RANGE EXPANSION PATTERNS

There are many case histories of species that were brought from one country to another and explosively proliferated in their new habitat (see Elton 1958; Crosby 1986; Mooney and Drake 1986; Kornberg and Williamson 1987; Okubo 1988; Drake et al. 1989; Hengeveld 1989; Lodge 1993). The following examples of mammal, bird, insect, and plant species, for which the progress of invasion is well documented, show typical patterns of range expansions.

One of the best-known examples of spread is the North American muskrat, *Ondatra zibethica,* which was released near Prague in 1905. The contour map that documents the spread of this population in central Europe from 1909 to 1927 was illustrated by Elton (1958) based on Ulbrich's work (1930). Skellam (1951) analyzed the data and observed that the square root of the area occupied by this population increased as an approximately linear function of time. Skellam also demonstrated that the constant rate of range expansion could be explained by a simple diffusion equation combined with population growth. Recently, Andow et al. (1990, 1993) tested Skellam's prediction for muskrat spread by applying locally measured demographic and behavioral parameters and confirmed that agreement between theory and observation is good. A leading edge of the invasion progressing at a constant velocity is frequently observed in some other mammals and insects (Rapoport 1983; Thresh 1983; Andow et al. 1993). For example, Lubina and Levin (1988) found that the range expansion of the sea otter (*Enhydra lutris*) along the California coastline increased linearly with time.

A typical example of avian range expansion is the geographical invasion of the

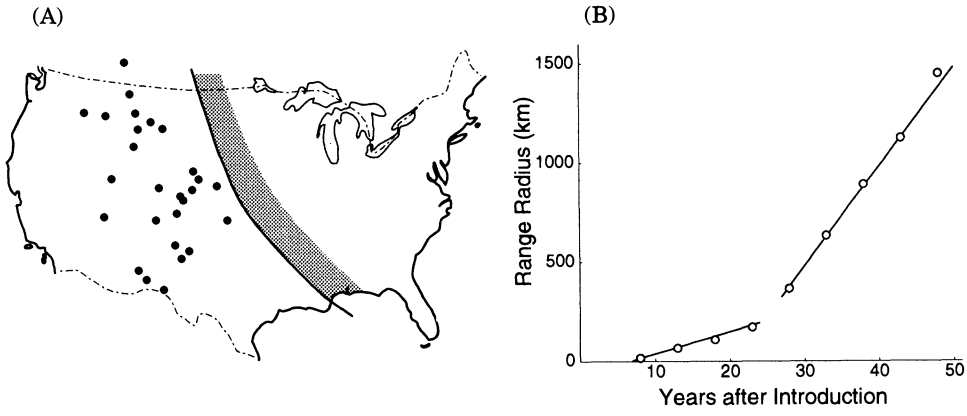

FIG. 1.—The range of the European starling in North America in 1941. *A*, The region to the right of the bold line is the breeding range, and the dots indicate where young overwintering birds without territories were found (redrawn from Hengeveld 1989); *B*, the range-versus-time curve (after Okubo 1988).

European starling (*Sturnus vulgaris*) in the United States. In 1891, 160 birds were released in Central Park, New York City. However, it took about 10 yr for the species to become established around the city. Figure 1*A* illustrates the range observed in 1941. The region to the right of the bold line is the breeding range, and the dots outside the breeding range indicate young overwintering birds that had previously failed to establish their territories (Hengeveld 1989). These latter birds served as bridgeheads from which further neighborhood expansion of the breeding range has occurred. Okubo (1988) plotted the progress of the range radius (the square root of the breeding area divided by $\sqrt{\pi}$) as a function of time (fig. 1*B*). Before 1900, there was no range expansion. From 1900 to 1915, the spread was gradual (11.2 km/yr) and then accelerated to a higher constant rate (51.2 km/yr).

The English sparrow and the house finch are also successful North American invaders. The expansions of these birds show similar trends in that they exhibit an initial establishment phase followed by expansion at a slow rate and then a steep linear range-versus-time curve in the later stage (Okubo 1988).

The rice water weevil (*Lissorhoptrus orzyzophilus*), first discovered in the central part of Japan in 1976, spread over the whole mainland during the next 10 yr, becoming one of the greatest threats to rice production in Japan (Tsuzuki and Isogawa 1976; Iwata 1979; Kiritani 1984). Andow et al. (1993) divided the area of occupation into three sectors—north, northeast, and west—and evaluated the range and rate of spread with time, as shown in figure 2. In contrast to the spread of muskrat and avian species, the rice water weevil does not show a phase of linear expansion with time. Instead, the rate of spread appears to be continually increasing. The acceleration of spread rate in this species could be related to its dispersal behavior. Rice water weevil disperses in two ways: by crawling and swimming from paddy to paddy and by flying. Andow et al. (1993) pointed out

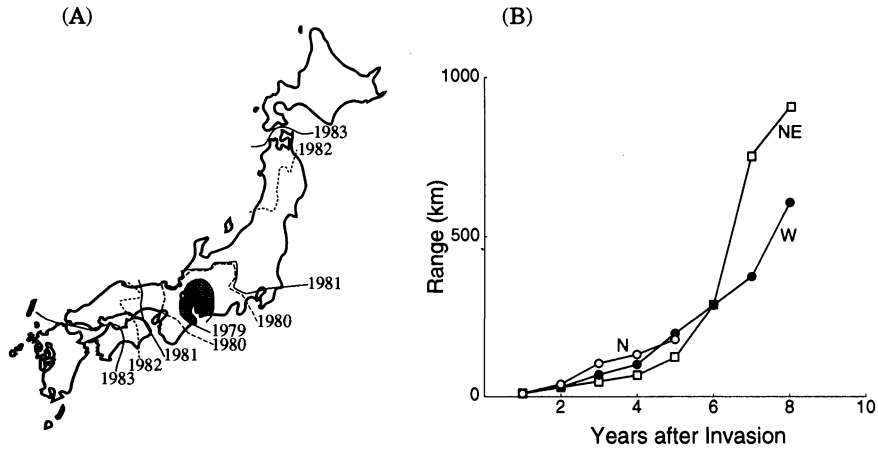

FIG. 2.—*A*, Spread of the rice water weevil, which was first found at Nagoya in 1976 and spread over mainland Japan in 10 yr; *B*, the range-versus-time curve. Solid circles indicate westward expansion, open circles indicate northward expansion, and open squares indicate north-eastward expansion (redrawn from Andow et al. 1993).

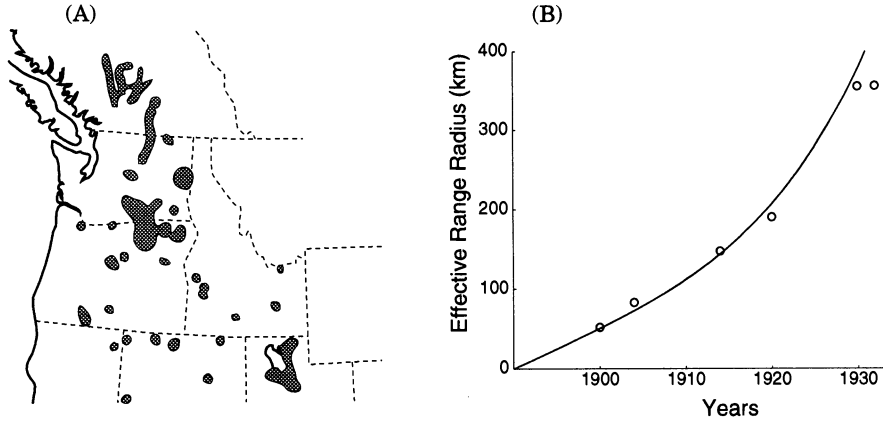

FIG. 3.—*A*, Geographical expansion of cheat grass in western North America, 1915–1920 (redrawn from Mack 1981); *B*, the effective range radius as a function of time. The open circles indicate data taken from Mack (1981), and the solid line depicts a theoretical curve derived from the scattered colony model.

that if relatively few beetles fly long distances, then early observations of spread rate will mostly reflect the short-distance dispersal, while later observations will be affected by the few pioneering beetles that underwent long-distance dispersal and whose offspring became abundant enough after a certain lag of time.

The last example is the spread of cheat grass (*Bromus tectorum*) into western North America as documented by Mack (1981, 1985, 1986). Cheat grass was found only at scattered locations between 1882 and 1900, after which both the number of locations and their population size increased exponentially (see fig. 3*A*).

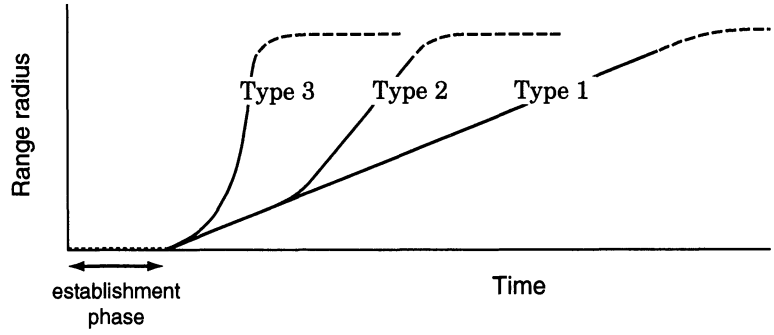

FIG. 4.—Three types of range-versus-time curves. Range expansion patterns commonly have an establishment phase (*arrow*), expansion phase (*solid line*), and saturation phase (*dashed line*), successively. The expansion phase is classified into three types. Type 1 shows linear expansion. Type 2 exhibits biphasic expansion, with an initial slow slope followed by a steep linear slope. In type 3, the rate of expansion continually increases with time.

In 40 yr, the area occupied by *Bromus* reached more than 200,000 km^2 in the intermountain west of North America, and at present it is the sole dominant in ranges and fields. Mack (1981) noted that formation of nuclei of isolated colonization at large distances from the parent population could enhance spatial spread considerably. The scattered nuclei may have been generated in part by human transportation facilities such as horse-drawn carriages and railroad systems (the latter were completed at the end of the nineteenth century). Figure 3*B* illustrates the effective range radius as a function of time. The rate of spread was approximately 5 km/yr in the early stage, and it continually increased in the later stage, until the range reached a saturation phase around 1930.

Thus far, we have considered various patterns of range expansions in terms of the range-versus-time curves (the range is defined as the square root of the invaded area divided by $\sqrt{\pi}$ or as the average total expanding length after Andow et al. 1993), which can be qualitatively classified into three types, as shown in figure 4. All three types have in common the initial establishment phase, during which no range expansion is discernible, followed by an expansion phase and then the final saturation phase, if there is a geographical limit to expansion. If we focus on the expansion phase, the patterns are further divided into three categories. In type 1, the range always expands linearly with time, as seen in the muskrat population. The expansion phase of type 2 includes a slow initial spread followed by linear expansion at a higher rate, as seen with the European starling. In type 3, the spread rate is continually increasing with time and forms a convex curve. The rice water weevil and cheat grass exemplify this type of expansion.

There could be many reasons for the occurrence of the establishment phase. For example, invading organisms may be ill adapted to the new environment and barely able to persist at low densities within the original colonizing area. Meanwhile, if offspring with a higher fecundity happen to evolve in the population, their range will start to expand. The lag period before the favorable mutant appears and successfully increases should correspond to the establishment phase. Another

more plausible reason may be that a few organisms initially released at a local point rapidly disperse so that they cannot be detected until their descendants reach a sufficiently high density. A mathematical model to investigate the latter case is presented in the following section.

The shape of the invasion curve in the expansion phase may depend on the life-history characteristics of each species. In fact, species belonging to each type appear to have common behavioral patterns with respect to their dispersal process. For example, in the populations of type 1, the offspring usually settle in the neighborhood of the range of their parent population. In contrast, species of types 2 and 3 can undergo long-distance dispersal as well as short-distance dispersal. Migration by short-distance dispersal expands the occupied area from its periphery, while long-distance dispersal generates new colonized patches far from the resident range. Thus, various types of range expansion may emerge depending on how short- and long-distance dispersal is involved in invasion.

RANGE EXPANSION BY NEIGHBORHOOD DIFFUSION

When the mean length of individual moves is not large, it is natural to model the dispersal process as a random walk (Okubo 1980; Murray 1989). The seminal model for range expansion due to short-distance dispersal was proposed by Skellam (1951) and was based on a diffusion equation combined with a Malthusian growth term, giving

$$\frac{\partial n}{\partial t} = D\left(\frac{\partial^2 n}{\partial x^2} + \frac{\partial^2 n}{\partial y^2}\right) + \epsilon n, \tag{1}$$

where $n(x, t)$ denotes the local population density at time t and the spatial coordinate $x = (x, y)$, D is the diffusion coefficient, and ϵ is the intrinsic growth rate of the population. Skellam examined equation (1) and showed that the rate of spread at the front of the range asymptotically approaches $2\sqrt{\epsilon D}$ when a small number of propagules is initially introduced at the center (for reviews see Okubo 1980; Murray 1989; Andow et al. 1993). On the other hand, Fisher (1937) and Kolmogorov et al. (1937) analyzed a diffusion equation combined with a logistic term $\epsilon(1 - n)n$ in the framework of population genetics and showed that any localized initial distribution of an advantageous gene evolves to a traveling frontal wave with a constant speed, $2\sqrt{\epsilon D}$, which coincides with the asymptotic speed derived by Skellam (see also Bramson 1973; Britton 1985).

Although Skellam's classic work is widely known, it has not been pointed out that the solution of equation (1) involves an initial establishment phase during which no range expansion is observed (but see Andow et al. 1993). Thus, we briefly summarize the results of his analyses and demonstrate how the range-versus-time curve of type 1 appears depending on the parameters of the model.

If N_0 propagules initially invade the center of the coordinate space, equation (1) is solved with the initial condition $n(x, 0) = N_0\delta(x)$ as

$$n(r,t) = \frac{N_0}{4\pi Dt}\exp\left(\epsilon t - \frac{r^2}{4Dt}\right), \tag{2}$$

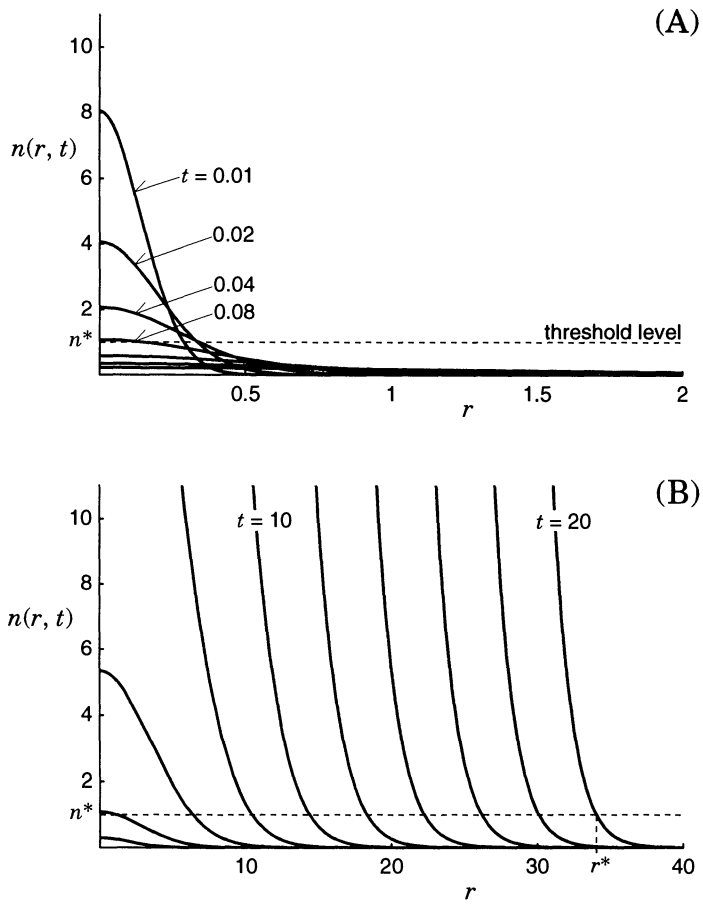

FIG. 5.—The solution of the Skellam model. The population initially released at the origin expands radially with time. The horizontal axis indicates radius r, and the vertical axis indicates the population density at radius r and at time t; $\epsilon = 1$, $D = 1$. *A*, Change in the distribution for $t = 0$–1; *B*, change in the distribution for $t = 2$–20. The dashed line indicates the threshold density, n^*, and r^* represents the range radius of the population.

where $\delta(x)$ is the delta function and r indicates the radial distance from the center, $r = (x^2 + y^2)^{1/2}$. Figure 5 illustrates how the spatial pattern spreads radially as time passes. In general, we regard a range as invaded if at least a few individuals are observed there. However, there could be a minimum density below which the population cannot be detected because of our limited searching ability. We denote such a threshold density by n^* and define the area in which $n(r, t) > n^*$ as the range of the population (Skellam 1951; Okubo 1980; Andow et al. 1990). Then the range radius denoted by r^* is the value of r at which the population density intersects the threshold level n^*. As seen in figure 5, the initial colonizing population immediately decreases below the threshold level due to diffusion,

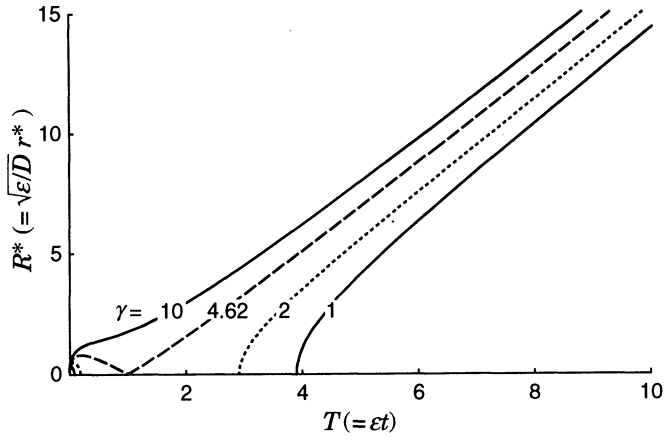

FIG. 6.—The range-versus-time relation as given by equation (4). The slope asymptotically approaches two for all values of γ. The establishment phase appears when γ is less than 4.62.

unless the threshold level n^* is very low. However, after a certain period, the population size gradually recovers to the threshold level by the reproduction process, and then the range starts to expand. This lag period may be regarded as the establishment phase. To see how the range radius r^* expands with time, we substitute $n = n^*$ and $r = r^*$ in equation (2) and rewrite it with nondimensionalized variables:

$$R^* = \sqrt{\frac{\epsilon}{D}}\,r^*, \quad T = \epsilon t, \tag{3}$$

and

$$\gamma = \frac{\epsilon N_0}{Dn^*},$$

whence

$$R^* = 2T\left(1 + \frac{1}{T}\log\frac{\gamma}{4\pi T}\right)^{1/2}. \tag{4}$$

This range-versus-time relation in the nondimensionalized version depends on only one parameter, γ. Figure 6 illustrates R^* as a function of T with varying values of γ. When γ is larger than $4\pi/e$ (≈ 4.62), the curve increases almost linearly with time, and the slope of the curve tends to $dR^*/dT = 2$. However, as γ decreases below $4\pi/e$, there appears an establishment phase followed by an expansion phase in which the expansion rate is approximately given by $dR^*/dT = 2$. If we revert to the original variables by using equation (3), the above result is reinterpreted in terms of actual dimensions as follows: when $\gamma = \epsilon N_0/Dn^* >$

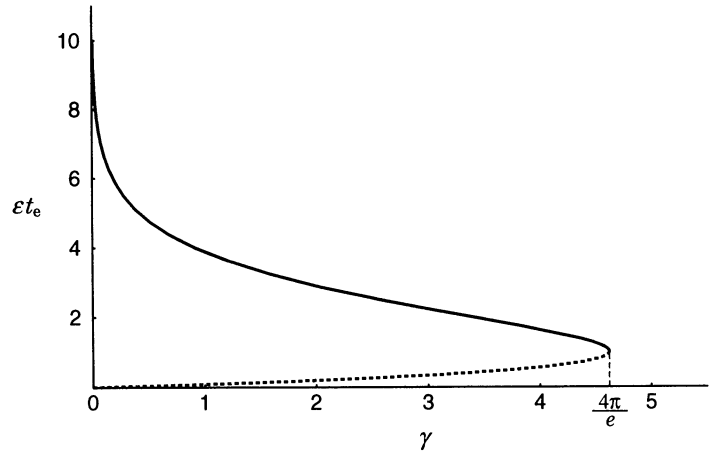

FIG. 7.—The length of establishment phase as a function of γ. The lag period t_e rapidly decreases as γ increases from zero, and when γ exceeds $4\pi/e$ ($\approx$4.62), t_e abruptly becomes zero. The dashed line represents the time taken for the density of initially released individuals to go below the threshold density as a result of dispersal.

$4\pi/e$, the range radius $r^*(t)$ starts to expand from the beginning, and the speed of the advancing front asymptotically approaches the constant rate $dr^*/dt = 2\sqrt{\epsilon D}$; when $\gamma = \epsilon N_0/Dn^* < 4\pi/e$, there exists a time lag during which establishment occurs and after which the range tends to expand at the constant rate $dr^*/dt \approx 2\sqrt{\epsilon D}$. The length of the establishment phase, t_e, is calculated by putting $R^* = 0$ and $T = \epsilon t_e$ in equation (4) to give

$$\gamma = 4\pi\epsilon t_e \exp(-\epsilon t_e) . \tag{5}$$

Figure 7 illustrates ϵt_e as a function of γ. The value of t_e is infinitely large when γ is close to zero, and it rapidly decreases with increases in γ. When γ reaches $4\pi/e$, t_e vanishes suddenly. In terms of the original parameters, the establishment phase is prolonged as N_0 and ϵ decrease or as n^* and D increase. If estimates of N_0, ϵ, t_e, and D are available, the threshold density n^* can be estimated from equation (5).

To see whether the above results are robust to modification of the growth term in equation (1), we numerically solved the diffusion equation with the growth term $\epsilon(1 - n/K)n$, the so-called Fisher equation, under the same initial condition as above. We found that the spatial pattern of the Fisher model changes in almost the same way as that of the Skellam model from the initial declining phase through the subsequent recovering phase, as seen in figure 5. Even after the frontal propagating wave has been established, the leading edges of the advancing front move at the same speed in both models, although the shapes behind the fronts are significantly different; that is, the density at the tail approaches the saturation level K in Fisher's model, while it explodes to infinity in Skellam's model. Thus, so long as the threshold density n^* is sufficiently small compared with K, the range-versus-time relation given by figure 6 still holds for the Fisher model. Simi-

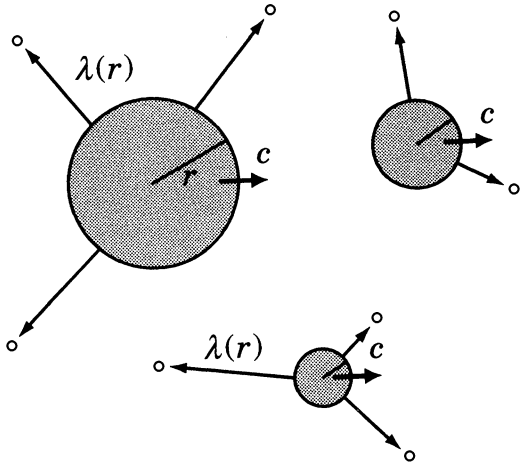

FIG. 8.—Range expansion in the scattered colony model. The invading species expands its range at a constant rate c by neighborhood diffusion and simultaneously produces long-distance dispersers that create nuclei of new colonization. Each nucleus expands at the constant rate c and at the same time emits long-distance dispersers, as does its parent population. Nuclei are far enough apart that they independently expand their ranges for a long time.

lar computations were carried out with other models, and we conclude that populations that expand by neighborhood diffusion together with appropriate reproductive growth will exhibit an invasion curve of type 1, although the duration of the establishment phase varies with parameter values.

INVASION BY STRATIFIED DIFFUSION

Scattered Colony Model

Let us consider a homogeneous environment in which an invading species is expanding its range by both neighborhood diffusion and long-distance dispersal. Here we focus on the special case in which nuclei of colonization created by long-distance migrants are located far enough from each other that their ranges do not overlap for a long time, as seen in the invasion of cheat grass (see fig. 8).

In the beginning, a few propagules invade a point and create there a nucleus of an isolated colony. The nucleus begins to expand its range by neighborhood diffusion. According to Skellam's work as summarized in the preceding section, the occupied area forms a disk shape centered at the initial point of invasion, and its radius tends to increase at the constant rate $c = 2\sqrt{\epsilon D}$, where ϵ is the intrinsic growth rate and D is the diffusion constant of this species. For simplicity, we assume that the length of the establishment phase is negligibly short so that the range radius begins to expand at the constant rate c immediately after nucleus formation. From the expanding colony, long-distance migrants are produced at the rate $k(r)$, where r is the range radius of the colony. Among the long-distance

migrants, a fraction α can successfully create new nuclei. Thus, the product of $k(r)$ and α gives the colonization rate, which is denoted by $\lambda(r) = \alpha k(r)$. In general, successful colonization is achieved only when at least a few organisms settle in the same region and succeed in producing their offspring against the risk of extinction due to demographic stochasticity, inbreeding depression, or any other causes (Leigh 1981; Iwasa and Mochizuki 1988; Burgman et al. 1993). Accordingly, rate $\lambda(r)$ is taken to represent the number of nuclei that overcome those various severe conditions. The successful nuclei expand their ranges, simultaneously producing long-distance migrants, as does their parent population. Repeating these processes can lead to an exponential increase in the number of isolated colonies concomitant with an accelerated expansion of the population.

To see how the ranges of individual colonies increase in total, we introduce a size distribution function of colonies as denoted by $\rho(r, t)$; $\rho(r, t)dr$ represents the number of colonies whose radii lie between r and $r + dr$. After summing the areas of all colonies, the total area of occupation is given by

$$A(t) = \int_0^\infty 2\pi r^2 \rho(r, t) dr \ . \tag{6}$$

Since the radius of each colony increases at a rate c, $\rho(r, t)$ satisfies the so-called von Foerster equation,

$$\frac{\partial \rho(r, t)}{\partial t} + c \frac{\partial \rho(r, t)}{\partial r} = 0 \ , \tag{7}$$

which is subject to the following initial and boundary conditions:

$$\rho(r, 0) = \delta(r) \tag{8}$$

and

$$c\rho(0, t) = \int_0^\infty \lambda(r) \rho(r, t) dr \ . \tag{9}$$

Equation (7) has been used to describe the evolution of size distribution, in which the age or height of organisms is taken as size (Nisbet and Gurney 1982; Hallam and Levin 1986; Metz and Diekmann 1986). In the present model, the size is the radius of a colony that grows at a constant rate c by means of neighborhood diffusion. Equation (8) means that the propagules initially introduced at a point create a nucleus of radius zero at time $t = 0$. The boundary condition shown in equation (9) indicates that the number of nuclei newly created at time t per unit time is the total rate at which the long-distance migrants succeed in colonization.

The colonization rate $\lambda(r)$ should be given by a nondecreasing function of radius r. We adopt the following three simple forms for the function:

$$\lambda(r) = \lambda_0 \ , \tag{10a}$$

$$\lambda(r) = \lambda_1 r \ , \tag{10b}$$

and

$$\lambda(r) = \lambda_2 r^2 \ , \tag{10c}$$

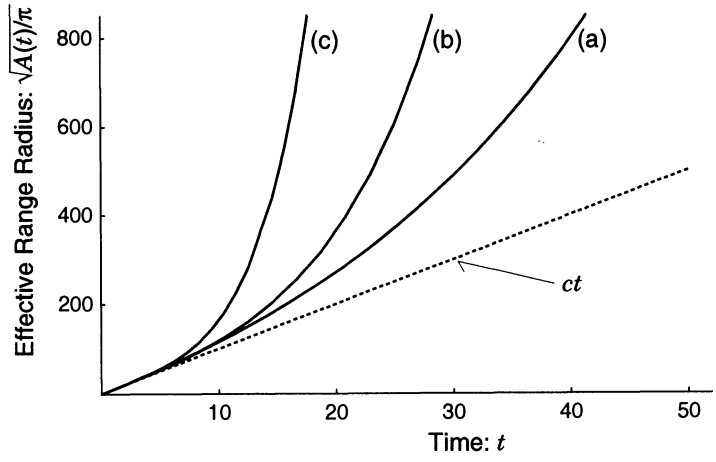

FIG. 9.—The range-versus-time curve obtained from the scattered colony model. The effective range radius is plotted from equation (11) for three different types of colonization rates. For line *a*, $\lambda(r) = 0.08$; for line *b*, $\lambda(r) = 0.004r$; and for line *c*, $\lambda(r) = 0.00004r^2$. The range initially expands at the constant rate *c* and then tends to increase exponentially for all cases, as is characteristic of a type 3 expansion curve.

which have the mechanistic implications described below. In equation (10a), every colony produces long-distance migrants at a constant rate, irrespective of its size. In equation (10b), long-distance migrants are produced in proportion to the circumference of the colonies. This may occur if the long-distance dispersers are produced only at the leading edge (or periphery) of each colony. In equation (10c), the production rate of long-distance dispersers per unit area is constant anywhere in the colony, so that the total rate per colony is proportional to its area.

For these typical forms of colonization rates, the total area occupied by the species is calculated by multiplying both sides of equation (7) by $2\pi r^2$ and then integrating the resultant with respect to r from 0 to ∞. Thus, the area-versus-time relations for equations (10a), (10b), and (10c) become (see app. A for derivation)

$$A(t) = \frac{2\pi c^2}{\lambda_0}\left(\frac{1}{\lambda_0}(e^{\lambda_0 t} - 1) - t\right), \tag{11a}$$

$$A(t) = \frac{\pi c}{\lambda_1}(e^{\sqrt{c\lambda_1}t/2} - e^{-\sqrt{c\lambda_1}t/2})^2, \tag{11b}$$

and

$$A(t) = \frac{2\pi c^2}{3\omega^2}\left(e^{\omega t} + 2e^{\omega t/2}\sin\left(\frac{\sqrt{3}}{2}\omega t - \frac{5}{6}\pi\right)\right), \tag{11c}$$

respectively, where $\omega = (2c^2\lambda_2)^{1/3}$. In figure 9, the effective range radii defined by $\sqrt{A(t)/\pi}$ for equations (11) are illustrated as functions of time. Each curve

shows accelerating increase, giving range-versus-time relations conforming to type 3. At the initial stage of invasion (i.e., when t is small), the effective range radii are approximated by ct for all cases, and they tend to increase exponentially in proportion to

$$\exp\{\lambda_0 t/2\}\,, \tag{12a}$$

$$\exp\{(c\lambda_1)^{1/2}t/2\}\,, \tag{12b}$$

$$\exp\{(2c^2\lambda_2)^{1/3}t\} \tag{12c}$$

for equations (10a), (10b), and (10c), respectively.

The above result is applied to the invasion of cheat grass shown in figure 3. As Mack (1981) noted, seeds of cheat grass were disseminated not only by animals but also by transportation facilities such as trains and horse-drawn carriages. If dispersal due to the transportation facilities plays a major role in long-distance dispersal, the seeds will disperse from almost anywhere within colonized areas. In such a case, equation (10c), $\lambda(r) = \lambda_2 r^2$, may be appropriate to describe the colonization rate. From figure 3, the effective range radius of cheat grass is approximated by $5(t - 1890)$ km/yr in the early stage. Thus, we have $c = 5$ km/yr for the propagating speed due to neighborhood diffusion. If we adopt $\lambda_2 = 3.5 \times 10^{-5}/\text{km}^2\ \text{yr}^{-1}$ for the colonization coefficient, the whole data obtained by Mack are fairly well fitted with a theoretical curve given by equation (11c), as illustrated by the solid curve in figure 3*B*. This means that cheat grass generates only 3.5×10^{-5} successful nuclei per square kilometer per year. It is surprising that such a small amount of nucleation is sufficient to cover the whole area of the western highland of America in two decades.

Coalescing Colony Model

When long-distance dispersers settle fairly close to their parent population, newly generated colonies will continue to expand in isolation for a short while, until they eventually merge with their parent population. To incorporate such a coalescing process, we develop a model that is simple enough to permit a partial analytical treatment.

As in the previous model, we assume that a few propagules of an alien species invade a local point at time $t = 0$. They immediately start to expand their range by neighborhood diffusion so that the occupied area maintains circular pattern with its radius expanding at the speed $c = 2\sqrt{\epsilon D}$ during the initial stage. We call this initially colonizing population the primary population and its range the primary colony. The primary population produces long-distance dispersers, some of which successfully settle at points located at a distance L ahead of the front of the primary colony (see fig. 10). The colonization rate is given by $\lambda(r)$ as defined in the previous section. Each new colony, which expands in a circular manner at a speed c, is referred to as an offspring colony. Since both the offspring and primary colonies are expanding, their ranges eventually collide with each other. We assume that, upon every event of collision, an offspring population coalesces into the primary population and the range of the combined colony is immediately reshaped in a circular pattern around the center of the primary col-

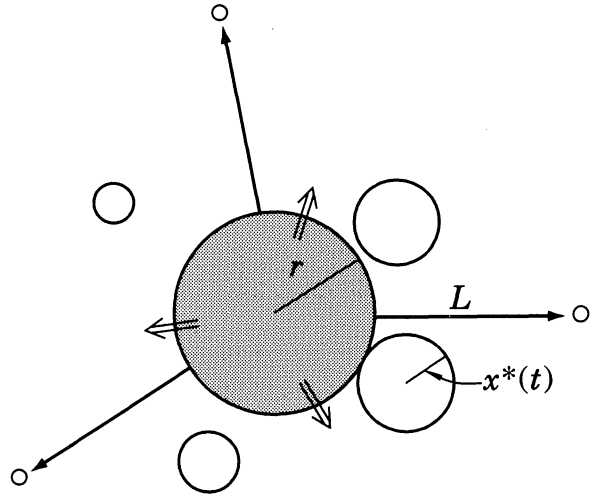

FIG. 10.—Range expansion in the coalescing colony model. The primary colony (*shaded circle*) expands its range by short-distance dispersal, and at the same time it emits long-distance migrants at the rate $\lambda(r)$, which settle at a distance L ahead of the front of the primary population. Each offspring colony that expands at the rate c coalesces into the primary population when their ranges overlap. Upon coalescence, the range of the primary colony including the offspring colony is immediately reshaped in a circular pattern, and the total area is unchanged.

ony with the total area kept unchanged. We also assume that coalescence between offspring colonies and secondary colonization by long-distance dispersers from offspring colonies rarely occur, although these effects will be taken into account in computer simulations as shown later. These assumptions may be permissible if the jump distance L is small enough that each offspring colony remains small until it coalesces.

To incorporate the coalescing processes, the scattered colony model given by equations (7)–(9) is modified as described below. Let $r(t)$ denote the range radius of the primary colony at time t, and $\rho(x, t)$ the size distribution function for offspring colonies as defined before. Then we have an equation similar to equation (7):

$$\frac{\partial \rho(x, t)}{\partial t} + c\frac{\partial \rho(x, t)}{\partial x} = 0 \quad \text{for } x^*(t) > x > 0 , \tag{13}$$

which is subject to the following initial and boundary conditions:

$$\rho(x, 0) = 0 \tag{14a}$$

and

$$c\rho(0, t) = \lambda(r) . \tag{14b}$$

In equation (13), the sizes of offspring colonies, x, lie between zero and $x^*(t)$, where $x^*(t)$ is the size of the offspring colony immediately before it merges with the primary colony at time t (see fig. 10). The initial condition given by equation

(14a) means that there is no offspring colony in the beginning. The boundary condition given by equation (14b) indicates that only the primary population is engaged in offspring colony formation. Equation (13) with equations (14) is solved as follows:

$$\rho(x, t) = \begin{cases} 0 & \text{for } x > ct > 0 , \\ \frac{1}{c}\lambda\left(r\left(t - \frac{x}{c}\right)\right) & \text{for } ct \geq x . \end{cases} \tag{15}$$

On the other hand, the dynamics of range expansion of the primary colony is given by the following equations:

$$\frac{d}{dt}\pi r^2 = \begin{cases} 2\pi rc & \text{for } t_s > t > 0 , \\ 2\pi rc + \pi x^{*2}\rho(x^*, t)(c - \dot{x}^*) & \text{for } t \geq t_s . \end{cases} \tag{16}$$

The left side represents the rate of change of the area of the primary colony. If the primary population emits long-distance dispersers immediately after it starts to expand at $t = 0$, both the primary and offspring colonies independently expand at a rate c until the first collision occurs at time $t_s = L/2c$. The upper equation of equation (16) describes the area expansion solely by neighborhood diffusion before the first collision occurs. When t exceeds t_s, the increase in the area is caused not only by neighborhood diffusion but also by the coalescence of the offspring colonies as given by the additional term in the second equation of equation (16), where the notation $\dot{x}^*(t)$ denotes differentiation with respect to t (see app. B for derivation). There is a relation between the range radius $r(t)$ of the primary colony and the maximum radius $x^*(t)$ of offspring colonies as

$$L = r(t) - r\left(t - \frac{x^*(t)}{c}\right) + x^*(t) \quad \text{for } t \geq t_s . \tag{17}$$

This equation implies that the offspring population having the maximum radius $x^*(t)$ at t settled at distance L ahead of the front of the primary population at time $t - x^*/c$, while the primary population has since expanded its range radius from $r(t - x^*/c)$ to $r(t)$ (see fig. 11). Thus, the total range expansion made by the primary and offspring colonies during x^*/c should be equal to L.

Combining equations (15) and (16) together with equation (17) completes the model for range expansion with coalescence, which involves two variables, $r(t)$ and $x^*(t)$. This set of equations can be rewritten in an alternative form. Differentiating equation (17) by t and substituting the resultant and equation (15) into equation (16) gives

$$\begin{cases} r(t) = ct & \text{for } t_s > t > 0 , \\ \dot{r} = \dfrac{2r(c + \dot{r}') + x^{*2}\lambda'}{2r(c + \dot{r}') - x^{*2}\lambda'}c & \text{for } t \geq t_s , \\ \dot{x}^* = \dfrac{c}{c + \dot{r}'}(\dot{r}' - \dot{r}) & \end{cases} \tag{18}$$

where

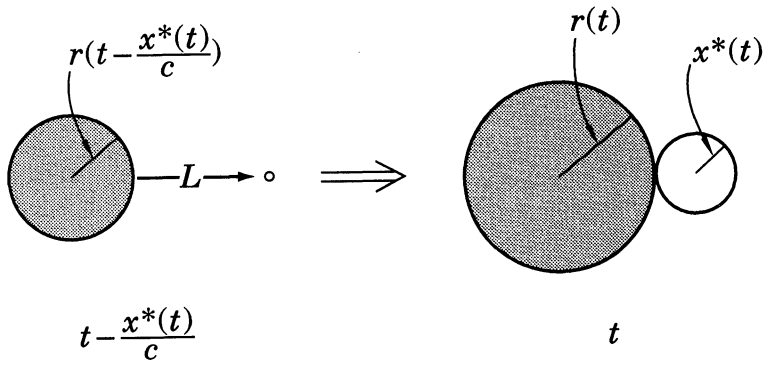

FIG. 11.—Growth of the primary and offspring colonies prior to their coalescence. Since this offspring population expands at a constant rate c, it should be generated at time $t - x^*/c$ from the primary colony whose radius was $r(t - x^*/c)$.

$$r' = r\left(t - \frac{x^*(t)}{c}\right) \text{ and } \lambda' = \lambda(r') .$$

We have solved equation (18) numerically, assuming $\lambda(r)$ to be given by equations (10). Typical curves of range radius for equations (10) are illustrated in figure 12. When t is less than t_s, $r(t)$ increases at the constant rate c for all cases, because there is no coalescence in that time interval. However, when $t > t_s$, the curves of $r(t)$ behave differently depending on the functional form of $\lambda(r)$. The characteristic properties of the range-time relations are summarized below.

First, when $\lambda(r) = \lambda_0$, $r(t)$ increases mostly at the constant rate c, although the rate of increase is slightly elevated just after t exceeds t_s. Thus, this case results in the range-versus-time relation of type 1.

Next, when $\lambda(r) = \lambda_1 r$, the slope of $r(t)$ switches from c to a higher value at $t = t_s$. The rate of change in $r(t)$ after t_s is almost constant, tending to an asymptote as t goes to infinity. Thus, the pattern of $r(t)$ is classified as type 2. The higher expansion rate is given as a function of the parameters c, L, and λ_1 as (see app. C)

$$\left.\frac{dr}{dt}\right|_{t\to\infty} = c + \frac{\lambda_1 x^*(\infty)^2}{2} , \tag{19}$$

where $x^*(\infty)$ is the positive solution of the following equation:

$$x^*(\infty)^3 + \frac{4c}{\lambda_1} x^*(\infty) - \frac{2cL}{\lambda_1} = 0 . \tag{20}$$

Thus, the expansion rate increases by $\lambda_1 x^*(\infty)^2/2$ after time t_s.

Finally, when $\lambda(r) = \lambda_2 r^2$, the expansion rate is continually accelerating after t_s and forms a type 3, range-versus-time pattern, although the curve shows slight oscillations with time. The oscillation is caused by the assumption that landing points of new colonizers concentrate on a circle separated by distance L from the front of the primary population.

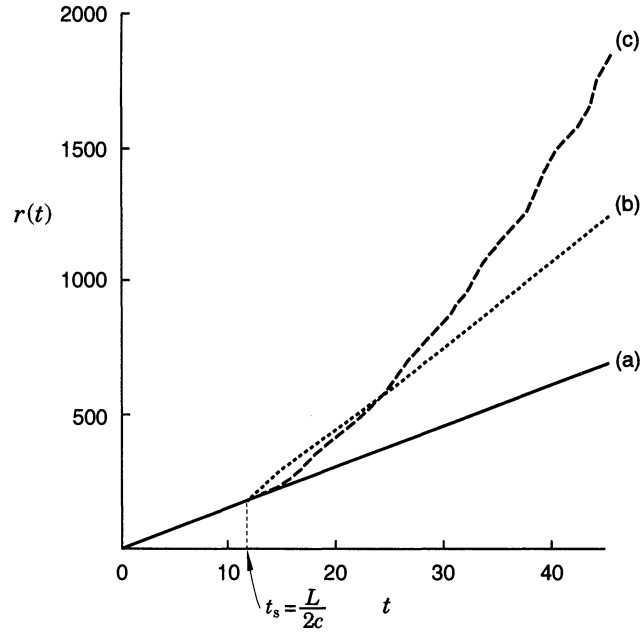

FIG. 12.—The range-versus-time curve obtained from the coalescing colony model. The range radius of the primary colony, $r(t)$, is calculated for the three types of colonization rates; c = 15 km/yr, and L = 400 km. For line a, $\lambda(r) = 0.01$, and $r(t)$ increases mostly at the rate of c, as is characteristic of a type 1 expansion curve; for line b, $\lambda(r) = 0.005r$, and $r(t)$ shows a type 2 biphasic expansion; for line c, $(r) = 0.00003r^2$, and $r(t)$ increases at accelerating rates, as is characteristic of a type 3 expansion.

Although we have dealt with only the three basic forms of $\lambda(r)$, it can be shown in general that, when $\lambda(r)$ increases with r in a greater than linear fashion (i.e., $\lambda(r)$ is a convex downward curve), $r(t)$ grows acceleratingly with time, so it is classified as type 3. On the other hand, when $\lambda(r)$ is given by a concave function such as r^θ with $0 < \theta < 1$, $r(t)$ is approximately a straight line, which is characteristic type 1 behavior. It can be concluded that the type 2 pattern is observed only when $\lambda(r)$ is proportional to r, that is, when new colonies are founded mainly by long-distance migrants that are born at the periphery of the range of the primary population.

If actual data that show the expansion pattern of type 2 are available, the values of the basic parameters of the invasion processes, c, L, and λ_1, can be estimated by the following procedure. First, the speed of expansion due to neighborhood diffusion, c, is evaluated from the initial speed. Then t_s can be determined by locating the point on the time axis where the switch occurs to a higher constant speed. If these values are substituted into the relation $L = 2ct_s$, the jumping distance of long-distance dispersal, L, is obtained. To derive the value of λ_1, we estimate $dr/dt(\infty)$ from the later elevated expansion rate and substitute it together with the estimated values of c and L into equations (19) and (20).

Application of these procedures to the expansion curve of European starlings as shown in figure 1 resulted in the following estimates of the parameter values:

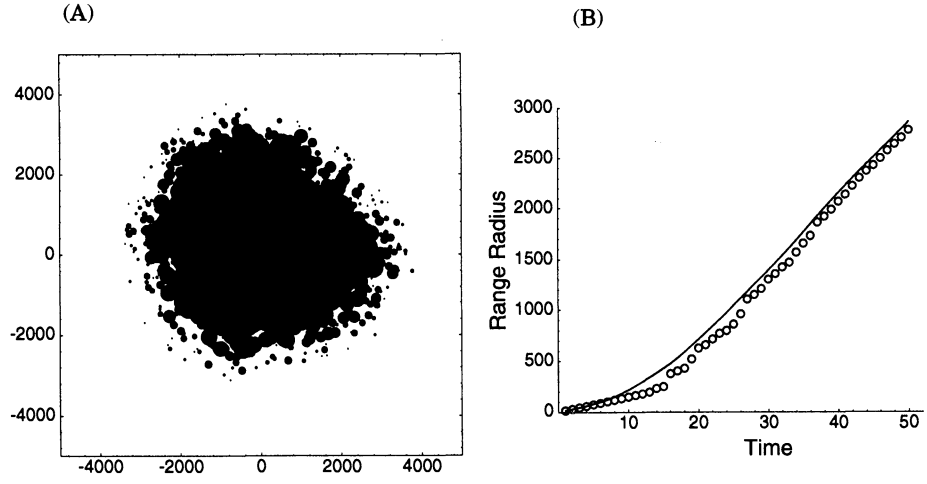

FIG. 13.—Computer simulation of the coalescing colony model for the colonization rate $\lambda(r) = 0.005r$; $c = 15$, $L = 400$. Offspring colonies expand their ranges without reshaping upon coalescence. The secondary colonization by offspring populations is also taken into consideration. *A*, Spatial distribution of colonies ($t = 50$); *B*, the range-versus-time curve. The open circles indicate the range radius of the primary colony, which shows biphasic expansion. The solid curve is the range radius of the total area, including the range of offspring colonies.

$c = 11$ km/yr, $L = 300$–400 km, $\lambda_1 \approx 0.02$/km yr^{-1}. As noted previously, the main range of European starlings was surrounded by young overwintering birds distributed in a belt zone of 300–800 km in width. If these young overwintering birds act as long-distance dispersers, their leap distance ranges 0–800 km, with a mean of 400 km. On the other hand, our model assumes that the jump distance of long-distance dispersers is concentrated at distance L ahead of the periphery of the primary range. If L is regarded as the mean of leap distances, the estimated value $L = 300$–400 km reasonably coincides with the one actually observed.

The rice water weevil, which exhibits a range-versus-time curve of type 3, expands its range by producing offspring colonies around the main population (see fig. 2). Thus, it represents another case of the coalescing colony model. Such a pattern of expansion could result if the long-distance migrants were generated at a rate proportional to the area of the primary colony and their flight distance were moderately long, so that new colonies quickly merged into the founder population.

In the coalescing colony model presented above, we ignored some important factors, such as time delay of expansion at the establishment phase, distributed settling locations of long-distance dispersers, secondary colonization by offspring populations, and coalescence of offspring colonies. Unfortunately, incorporation of such effects precludes further mathematical analyses. Thus, we carried out computer simulations in which coalescing colonies expand their ranges without reshaping and offspring populations are also permitted to generate long-distance dispersers (see fig. 13). Results of simulations exhibit invasion curves similar to those obtained from the corresponding analytical models in a qualitative sense: for the three cases of colonization rates as given by equations (10), invasion curves are of types 1, 2,

TABLE 1

CLASSIFICATION OF RANGE-VERSUS-TIME CURVES

	LEAP DISTANCE	
COLONIZATION RATE	Moderate	Long
λ_0	Type 1	Type 3
$\lambda_1 r$	Type 2	Type 3
$\lambda_2 r^2$	Type 3	Type 3

and 3, respectively. On close inspection, however, the invasion curves from simulation and analytical models differ from each other. In the simulation model, the rate of range expansion after $t = t_s$ for types 2 and 3 is higher than in the analytical model, if the parameter values are kept the same. We interpret these differences to mainly reflect extra contributions from secondary colonization by offspring population. The details of simulation analyses will be presented elsewhere.

Here it may be worthwhile to compare the present model with previous potentially relevant work. Mollison (1977) presented a spatial contact model, in which dispersal of juveniles is represented by the contact distribution function, which can formally incorporate any type of distribution for the distance of individual moves (see also Van den Bosch et al. 1990). In rough terms, our model may correspond to the special case in which the contact distribution function has two sharp peaks around jump distance, zero and L. However, the spatial contact model seems to be generally difficult to analyze except for contact distributions of simple functional forms. Articles somewhat related to the coalescing colony model were also presented to deal with the dynamics of expanding inhibitory fields, although those articles concerned competition for space rather than growth of colonies (Armstrong 1973, 1988; Glass 1973).

DISCUSSION AND CONCLUSIONS

In the preceding section, we have presented models for stratified diffusion to interpret three major types of invasion curves generally observed in nature. From analyses of the models, we found that the shape of the range-versus-time curve crucially depends on how and where short- and long-distance dispersers are produced and what distances they move (see table 1). Type 1 shows linear expansion and occurs only when dispersal is mainly mediated by neighborhood diffusion. On the other hand, species with short- and long-distance dispersers exhibit patterns of accelerated range expansions as indicated by types 2 and 3. Type 2 expansion, which is characterized by a biphasic expansion with an initial slow rate followed by a higher constant rate, appears when species produce long-distance migrants only at the periphery of the range and the long-distance migrants travel only moderate distances. Under these circumstances, the colonies founded by long-distance migrants will merge with the range of their parent population in a short time. In contrast, if species produce long-distance dispersers in proportion to the area of their ranges, they exhibit expansion curves with continually accelerating rates, as indicated by type 3. In this case, the flight length of long-distance

dispersers does not affect the pattern of type 3 qualitatively, as long as the length is large enough in comparison with that of short-distance dispersers.

The models presented here assume that the environment is homogeneous. In a heterogeneous habitat, however, the spread would not be radial, and the rate of spread should vary depending on variation in habitat (Andow et al. 1990). In particular, the growth dynamics of invading species are influenced by those of native species inhabiting local areas. When an invading species reaches a region already occupied by a competitively superior species, it would cease further advance or even retreat (Okubo et al. 1989). If the preoccupant species is the predator (parasite) or prey (host) of the invading species, the population dynamics could oscillate locally by prey-predator interaction (Murray et al. 1986; Murray 1989; Yachi et al. 1989; Comins et al. 1992). Studies have shown (Shigesada et al. 1986, 1987) that if the environment consists of favorable and unfavorable patches that are randomly distributed, invasion mediated by neighborhood diffusion can still be modeled by Skellam's equation in which habitat heterogeneity is incorporated by variations in D and ϵ. It was shown that although the range expands at varying speeds depending on which patch the front is passing, the averaged speed is approximated by $\langle c \rangle = 2\sqrt{\langle \epsilon \rangle_a \langle D \rangle_h}$, where $\langle \epsilon \rangle_a$ and $\langle D \rangle_h$ are the arithmetic mean of ϵ and the harmonic means of D over the space, respectively. Therefore, if we focus on the range expansion on a geographical scale in which favorable and unfavorable patches are distributed isotropically, we still can qualitatively interpret various types of range expansions by the present models if the propagating speed by neighborhood diffusion is substituted for the averaged speed $\langle c \rangle$ in the present models.

It should finally be remarked that the main focus of the present study is to propose simple and plausible models for explaining typical cases of stratified diffusion. If detailed quantitative data of dispersal became available for other species, their interpretations might need some modification or extension of the present models. We hope this work provides a starting point for such future investigations.

ACKNOWLEDGMENTS

We appreciate A. Okubo, D. Andow, and P. Kareiva for informing us of many important references on biological invasions. We also thank K. Aoki, A. Okubo, S. A. Levin, E. Holmes, J. Cohen, and H. Caswell for their valuable comments and suggestions. This work was supported by the Japan Ministry of Education, Science and Culture Grant-in-Aid for Scientific Research on Priority Areas project "Symbiotic biosphere: an ecological interaction network promoting the coexistence of many species" (no. 319). N.S. also acknowledges support of a Japan Ministry of Education, Science and Culture Grant-in-Aid for Scientific Research no. 06640818.

APPENDIX A

Derivation of Equation (11)

Let us define the following quantities,

$$N(t) = \int_0^\infty \rho(r, t)dr,$$
$$R(t) = \int_0^\infty r\rho(r, t)dr, \tag{A1}$$
$$A(t) = \int_0^\infty \pi r^2\rho(r, t)dr ,$$

where $N(t)$, $R(t)$, and $A(t)$ represent the total number, the total length of radii, and the total area, respectively, of colonies at time t. If we multiply the left side of equation (7) by πr^2, r, or 1 and integrate from 0 to ∞, the following equations are derived:

$$\frac{dA}{dt} - 2\pi cR = 0 ,$$
$$\frac{dR}{dt} - cN = 0 , \tag{A2}$$
$$\frac{dN}{dt} - c\rho(0, t) = 0 ,$$

where $\rho(0, t)$ is defined by equation (9), which is rewritten as a function of N, R, and A for three cases of equations (10) as follows:

$$c\rho(0, t) = \lambda_0 N , \tag{A3a}$$
$$c\rho(0, t) = \lambda_1 R , \tag{A3b}$$

and

$$c\rho(0, t) = \lambda_2 A/\pi . \tag{A3c}$$

Substituting equation (A3a), (A3b), or (A3c) into equation (A2) yields dynamical systems of N, R, and A for the case in which the colonization rate is given by equation (10a), (10b), or (10c), respectively. By solving those dynamical systems with the initial conditions, $N(0) = 1$, $R(0) = A(0) = 0$, we obtain equations (11).

APPENDIX B

Derivation of Equation (16)

Let $x^*(t)$ denote the radius of an offspring colony that just comes in contact with the primary colony at time t (see fig. 10). Then, offspring colonies expanding in isolation have radii smaller than $x^*(t)$. Among them, colonies of radius ranging between $x^*(t + dt) - cdt$ and $x^*(t)$ will coalesce with the primary one during $(t, t + dt)$, because the offspring upon collision at $t + dt$ has a radius of $x^*(t + dt)$ that has been growing at rate c from time t to $t + dt$. Thus, the total number of offspring colonies coalesced during $(t, t + dt)$ is given by $\rho(x^*, t)\{x^*(t) - (x^*(t + dt) - cdt)\} + 0(dt^2)$. Therefore, the increase of the primary colony's area by coalescence during dt is $\pi x^{*2}\rho(x^*, t)\{x^*(t + dt) - cdt - x^*(t)\} + 0(dt^2)$. Dividing the increment by dt and assuming dt tends to zero, we have $\pi x^{*2}\rho(x^*, t)(dx^*(t)/dt - c)$ as given in equation (16).

APPENDIX C

Derivation of Equation (19)

Assume that dr/dt converges to α (constant) at $t \to \infty$. Then from the last equation of equations (18), we have $\dot{x}^*(\infty) = 0$. Thus, x^* converges to a constant $x^*(\infty)$, because $0 < x^*(t) < L/2$ for all t. Substituting these relations and $\lambda(r) = \lambda_1 r$ into equations (15)–(17) leads to

$$\dot{r}(\infty) = \alpha = c + \frac{\lambda_1}{2} x^*(\infty)^2 ,$$

$$L = \frac{\alpha}{c} x^*(\infty) + x^*(\infty) . \tag{C1}$$

By eliminating α from the above equations, we have

$$x^*(\infty)^3 + \frac{4c}{\lambda_1} x^*(\infty) - \frac{2cL}{\lambda_1} = 0 . \tag{C2}$$

LITERATURE CITED

Andow, D., P. Kareiva, S. A. Levin, and A. Okubo. 1990. Spread of invading organisms. Landscape Ecology 4:177–188.

———. 1993. Spread of invading organisms: patterns of spread. Pages 219–242 *in* K. C. Kim, ed. Evolution of insect pests: the pattern of variations. Wiley, New York.

Armstrong, R. A. 1973. Dynamics of expanding inhibitory fields. Science (Washington, D.C.) 183: 444–445.

———. 1988. The effect of disturbance patch size on species coexistence. Journal of Theoretical Biology 133:169–184.

Bramson, M. 1973. Convergence of solutions of the Kolmogorov equation to travelling waves. AMS Memoirs, no. 285. Vol. 44. American Mathematical Society, Providence, R.I.

Britton, N. F. 1985. Reaction-diffusion equations and their applications to biology. Academic Press, London.

Burgman, M. A., S. Ferson, and H. R. Akcakaya. 1993. Risk assessment in conservation biology. Population and community biology series. Vol. 12. Chapman & Hall, London.

Cliff, A. D., P. Haggett, J. D. Ord, and G. R. Versey. 1981. Spatial diffusion. Cambridge University Press, Cambridge.

Comins, H. N., M. P. Hassell, and R. M. May. 1992. The spatial dynamics of host-parasitoid systems. Journal of Animal Ecology 61:735–748.

Crosby, A. W. 1986. Ecological imperialism: the biological expansion of Europe, 900–1900. Cambridge University Press, Cambridge.

Drake, J. A., H. A. Mooney, F. di Castri, R. H. Groves, F. J. Kruger, M. Rejmanek, and M. Williamson, eds. 1989. Biological invasions: a global perspective. Scope 37. Wiley, Chichester.

Elton, C. S. 1958. The ecology of invasion by animals and plants. Methuen, London.

Fisher, R. A. 1937. The wave of advance of advantageous genes. Annals of the Eugenics Society (London) 7:255–369.

Glass, L. 1973. Stochastic generation of regular distributions. Science (Washington, D.C.) 180: 1061–1063.

Hallam, T. G., and S. A. Levin, eds. 1986. Mathematical ecology: an introduction. Springer, New York.

Hengeveld, B. 1989. Dynamics of biological invasions. Chapman & Hall, London.

Holmes, E. E., M. A. Lewis, J. E. Banks, and R. R. Veit. 1994. Partial differential equations in ecology: spatial interactions and population dynamics. Ecology 75:17–29.

Iwasa, Y., and H. Mochizuki. 1988. Probability of population extinction accompanying a temporary decrease of population size. Researches on Population Ecology (Kyoto) 30:145–164.

Iwata, T. 1979. Invasion of the rice water weevil, *Lissorhoptrus oryzae* Kuschel, into Japan, spread of its distribution and abstract of the research experiments conducted in Japan. Japanese Pesticide Information 367:14–21.

Kiritani, K. 1984. Colonizing insects: colonist as a member of native insect community. Insekutariumu (Insectariume) 9:248–262.

Kolomogorov, A., N. Petrovsky, and N. S. Picoounov. 1937. A study of the equation of diffusion with increase in the quantity of matter, and its application to a biological problem. Moscow University Bulletin of Mathematics 1:1–25.

Kornberg, H., and M. H. Williamson, eds. 1987. Quantitative aspects of the ecology of biological invasions. Royal Society, London.

Leigh, E. G., Jr. 1981. The average lifetime of a population in a varying environment. Journal of Theoretical Biology 90:213–239.

Lodge, D. M. 1993. Biological invasion: lessons for ecology. Trends in Ecology & Evolution 8: 133–137.

Lubina, J. A., and S. A. Levin. 1988. The spread of a reinvading species: range expansion in the California sea otter. American Naturalist 131:526–543.

Mack, R. N. 1981. Invasion in *Bromus tectorum* L. into western North America: an ecological chronicle. Agro-Ecosystems 7:145–165.

———. 1985. Invading plants; their potential contribution to population biology. Pages 127–142 *in* J. White, ed. Studies in plant demography. Academic Press, London.

———. 1986. Alien plant invasion into the intermountain west: a case history. Pages 191–213 *in* H. A. Mooney and J. D. Drake, eds. Ecology of biological invasions of North America and Hawaii. Springer, New York.

Metz, J. A. J., and O. Diekmann. 1986. The dynamics of physiologically structured populations. Springer, New York.

Mollison, D. 1977. Spatial contact models for ecological and epidemic spread. Journal of the Royal Statistical Society B 39:283–326.

Mooney, H. A., and J. A. Drake, eds. 1986. Ecology of biological invasions of North America and Hawaii. Springer, New York.

Murray, J. D. 1989. Mathematical biology. Springer, New York.

Murray, J. D., E. A. Stanley, and D. L. Brown. 1986. On the spatial spread of rabies among foxes. Proceedings of the Royal Society of London B, Biological Sciences 229:111–150.

Nisbet, R. M., and W. S. C. Gurney. 1982. Modelling fluctuating populations. Wiley, Chichester.

Okubo, A. 1980. Diffusion and ecological problems: mathematical models. Springer, New York.

———. 1988. Diffusion-type models for avian range expansion. Pages 1038–1049 *in* H. Ouellet, ed. Acta XIX Congress Internationalis Ornithologici. Vol. 1. National Museum of Natural Sciences, University of Ottawa Press, Ottawa.

Okubo, A., P. K. Maini, M. H. Williamson, and J. D. Murray. 1989. On the spatial spread of the gray squirrel in Britain. Proceedings of the Royal Society of London B, Biological Sciences 238:113–125.

Rapoport, E. 1983. Aereography. Pergamon, Oxford.

Shigesada, N., K. Kawasaki, and E. Teramoto. 1986. Traveling periodic waves in heterogeneous environments. Theoretical Population Biology 30:143–160.

———. 1987. The speeds of traveling frontal waves in heterogeneous environments. Pages 88–97 *in* E. Teramoto and M. Yamaguti, eds. Population biology, morphogenesis and neurosciences. Lecture notes in biomathematics. Vol. 71. Springer, Heidelberg.

Skellam, J. G. 1951. Random dispersal in theoretical populations. Biometrika 38:196–218.

Thresh, J. M. 1983. Progress curves of plant virus disease. Advances in Applied Biology 8:1–85.

Tsuzuki, H., and Y. Isogawa. 1976. The first record of the rice water weevil, tentatively identified as *Lissorhoptrus oryzophilus,* in Aiti Prefecture, Japan (in Japanese). Syokubutu Boeki 30:341.

Ulbrich, J. 1930. Die Bisamratte. Heinrich, Dresden.

Van den Bosch, F., J. A. J. Metz, and O. Diekmann. 1990. The velocity of spatial population expansion. Journal of Mathematical Biology 28:529–565.

Yachi, S., K. Kawasaki, N. Shigesada, and E. Teramoto. 1989. Spatial patterns of propagating waves of fox rabies. Forma 4:3–12.

Associate Editor: Peter Chesson